Yielding and Flow Liquefaction of Loose Sand

S. M. Reza Imam[1], Norbert R. Morgenstern[2], Peter K. Robertson[3] and Dave H. Chan[3]

Corresponding author:
Norbert R. Morgenstern
Department of Civil and Environmental Engineering
University of Alberta, Edmonton, Alberta, Canada, T6G 2G7

submitted to
Soils and Foundations
Paper No. 2581

Submitted: Nov 27, 2000
Revised: September, 2001

---

1 Former post-doctoral fellow, University of Alberta; Faculty member, Shahid Chamran University, Ahvaz, Iran
2 University Professor, Department of Civil and Environmental Engineering, University of Alberta
3 Professor, Department of Civil and Environmental Engineering, University of Alberta

YIELDING AND FLOW LIQUEFACTION OF LOOSE SAND

Abstract

The relationship between the shapes of the yield surface and the undrained effective stress path (UESP) of loose sand is investigated for triaxial loading conditions. It is shown that the UESP can be used in the construction of capped yield surfaces for sands. The stress ratio M_p, measured at a point where the UESP of loose sand reaches a peak, has been incorporated as a material parameter in the analytical relationship by which the yield surface is defined. The variations of M_p with void ratio, state parameter, and consolidation stresses are examined and compared with previous studies, in cases where such studies exist. It is shown that M_p is strongly influenced by soil dilatancy and anisotropy and its variation is remarkably consistent with the variation of soil strength and yielding stresses. Quantitative relationships for the variations of M_p are then introduced and have been used elsewhere in constructing yield surfaces and modeling the constitutive behavior of sands. In addition to their use in modeling sand behavior, yield surfaces and quantitative variations of M_p obtained here can be used in quantitative assessments of the susceptibility of loose sandy soils to flow liquefaction.

key words: Sand; yield surface; constitutive Modeling; liquefaction; flow; instability, slope stability (IGC: D06; E06; E07)

INTRODUCTION

Establishing yield surfaces of sands from stress-strain data, and determining effects of various factors such as density, consolidation stresses, anisotropy, fabric etc. on the yielding behavior are not easy tasks. Construction of yield surfaces often requires tests in which complex and unconventional stress paths are imposed on the soil. In many instances, determination of stresses at which yielding occurs from stress-strain data requires considerable approximations. Moreover, loading soils often causes changes in their properties, making it difficult to reach different yield points belonging to the same yield locus, while the soil has a constant value of a certain property (e. g. void ratio, anisotropy, fabric, etc.). For clays, ellipses have often been used as yield surfaces while for sands, the more complex yielding behavior in addition to the difficulties cited above have led to the use of a wide range of shapes for yield surfaces, many of which depict actual yielding of sands only approximately.

Nova and Hueckel (1981) noted that very loose liquefiable sands experience no hardening due to shear strain; and, the amount of shear hardening increases with density. Lade (1992) suggested that in a plane of deviatoric stress $q = \sigma_1-\sigma_3$ vs mean normal stress $p = (\sigma_1+\sigma_2+\sigma_3)/3$, the peak point of the UESP of loose sands (P-UESP) occurs slightly after but very close to the peak point of the yield surface (P-YS). If the above propositions are verified experimentally, the UESP of loose sand can be utilized in the construction of yield surfaces. Since UESP's can be obtained readily by conventional tests and a large database of such tests is available in the literature, material parameters needed for the construction of yield surfaces and modeling sand behavior can be obtained easily from such data.

The state of stress at the P-UESP of loose sand has been examined frequently in the context of flow liquefaction over the past three decades (see eg. Bishop, 1971; Hanzawa, 1980; Vaid and

co-workers, 1985, 1995, 1999; Sladen et al., 1985; Lade and co-workers, 1992, 1993, 1997; Doanh et al., 1997). These studies have shown that the stress ratio q/p at the P-UESP, denoted by M_p here, is affected by void ratio, consolidation stresses, pre-shearing, direction of loading and soil anisotropy. Such investigations have often been limited to qualitative demonstrations of the influence of one or a number of these factors on M_p. In some recent studies, plots of variations of M_p with some of these factors have also been presented. However, in a quantitative assessment of the susceptibility of loose sand to flow liquefaction, numerical values of this stress ratio are needed in order to calculate the factor of safety against flow failure (see eg. Lade, 1993). Therefore, relationships which relate M_p to the factors that affect it need to be developed using independent test data. Such relationships are also required if stress states at the P-UESP are to be used in the construction of yield surfaces as discussed above.

In this paper, an analytical equation is introduced for the yield surface of sand and is verified against experimental yielding stresses of isotropically consolidated (IC) and anisotropically consolidated (AC) sand. The yield surface of loose Ottawa sand is then obtained using available test data, and then compared to the shape of the UESP. It is shown that shapes of the UESP and the YS, and the stress ratios M at their peaks, are very close to each other. It is also shown that the stress ratios at the P-YS and at the P-UESP are influenced by similar factors and that their variations with these factors are similar. We will therefore use the same notation M_p to represent both stress ratios.

Relationships by which variations of the stress state at the P-UESP can be modeled, are then obtained. These relationships describe a model, which is derived from the examination of an extensive body of published data. The model is presented partly in this paper for triaxial loading conditions and further extended and generalized to account for the effects of intermediate

principal stress and direction of loading in a companion paper (Imam et al., 2002). These relationships are used elsewhere to construct YS's which are employed in modeling the constitutive behavior of sands. The yield surfaces also provide quantitative criteria for assessing the susceptibility of loose sandy soils to flow liquefaction and can account for the factors influencing such susceptibility (see Imam, 1999).

Previous Studies on the Variation of M_p with Void Ratio and Consolidation Stresses

Bishop (1971) showed that the mobilized friction angle at the P-UESP of loose sand decreases with initial void ratio e_i and is smaller in Triaxial Extension (TE) compared to Triaxial Compression (TC). Based on results of TC tests on water pluviated (WP) samples, Vaid and Chern (1985) indicated that the stress ratio at the P-UESP, to which they referred as the "critical stress ratio (CSR)," is unique for a certain sand and corresponds to a friction angle close to φ_μ between soil particles. In subsequent studies, Vaid and co-workers (eg 1989, 1995, 1999) verified the uniqueness of the CSR in TC but showed that in TE and simple shear, CSR's may correspond to smaller friction angles and are functions of the initial void ratio e_i.

Lade (1992) noted that peak points of UESP's of samples prepared at the same e_i lie on a straight "Instability Line," which passes through the origin of the p-q plane, and is very close to a line connecting the top points of yield surfaces. Lade (1993) showed that for the TC data he examined, the friction angle φ_i corresponding to the instability line increases with the initial relative density Dr_i, and that the variation can be approximated by a curve. Later, Yamamuro and Lade (1997) showed that φ_i decreases with void ratio at consolidation e_c. Bopp and Lade (1997) conducted high pressure, undrained TC and TE tests on dry pluviated sand with Dr_i

ranging form 30% to 90% and consolidation pressures from 8 to 60 MPa. They indicated that the slope of the instability line increases slightly with decrease in void ratio, which is in turn caused by change in soil gradation due to particle crushing. Doanh et al. (1997) showed that the concept of instability line is also applicable to TE and AC sand. They indicated that anisotropic consolidation of sand does not affect the slope of the instability line if conducted along a stress ratio smaller than the instability line; otherwise, it increases the slope of the instability line.

Konrad (1993) obtained a unique stress ratio at the P-UESP for sand samples consolidated to the same void ratio but various pressures, and also for samples consolidated to the same pressure but various void ratios.

Lade and Yamamuro (1997) demonstrated the importance of fines content on the susceptibility of sand to flow liquefaction, and the effect of void ratio on the behavior of silty sands. However, the current study is limited to the behavior of clean sands.

SHAPE OF THE YIELD SURFACE OF SAND

Yield surfaces derived from stress-strain behavior of sands often resemble curves in the p-q plane which emanate from the origin and, after reaching a peak, bend towards the p-axis to form a cap (see e. g. Nova and Wood 1978; Yasufuko et al., 1991). Based on these results, the following function, which produces such shape, is postulated as the yield surface of IC sands, and is verified later against test results:

$$f = \eta^2 - k^2\left[1 - \left(\frac{p}{p_c}\right)^{\frac{1}{2}}\right] = 0 \qquad (1)$$

in which $\eta = q/p$ is the current stress ratio, p_c is the maximum value of p, and k is a material parameter. Yield functions having similar analytical forms and/or geometric representations

have been used frequently in constitutive modeling of sand recently (see e. g. Pestana-Nascimento 1994; di Prisco et al., 1993).

Representation of this yield function in the p-q plane exhibits a peak (see Figure 1), which is obtained by applying $\frac{dq}{dp} = 0$, from which the following relationship is obtained:

$$k^2 = 5\, M_p^{\,2} \tag{2}$$

in which M_p is a material parameter corresponding to the stress ratio at P-YS.

Stress ratios at P-YS on the compression side ($M_{p,c}$) and on the extension side ($M_{p,e}$) may not be the same. Figure 1 compares the yield surface defined by Equation 1 with the yield stresses obtained experimentally by Yasufuko et al. (1991) from tests on dense Aio sand. The solid lines in Figure 1 are obtained by substituting for $M_{p,c} = 1.015$ and $M_{p,e} = -0.758$ in Equation 1. These values were selected following Yasufuko et al. (1991) who used the same mobilized friction angle at P-YS in TC and TE. Figure 1 indicates that while the agreement between measured and modeled yielding stresses on the compression side is very good, yielding stresses on the extension side are substantially overestimated. Use of $M_{p,e} = -0.5$ shown by the broken line led to a significantly improved estimate of yielding stresses. Apart from the effect of the intermediate principal stress, which may slightly affect the friction angle at yielding in extension, the observed decrease in the friction angle on the extension side can be attributed to soil anisotropy.

Equation 1 can be modified to account for anisotropic consolidation. Experiments indicate that in triaxial plane, yield surfaces of AC sands rotate in the direction of consolidation (see eg Cambu and Lanier 1988; Yasufuko et al. 1991). Therefore, the point at which $dq/dp = \infty$ (i. e. where $p = p_c$ in IC sand) moves away from the p-axis and lies on a line corresponding to a stress ratio α. The mean normal stress at this stress ratio, p_α, is the largest yielding stress and is larger

than the consolidation pressure p_c. The stress ratio α is a measure of stress-induced anisotropy and may change during shearing, especially when the direction of shearing is reversed.

Equation 1, takes the following form for AC sand:

$$f = (\eta - \alpha)^2 - k^2 \left[1 - \left(\frac{p}{p_\alpha} \right)^{\frac{1}{2}} \right] = 0 \qquad (3)$$

in which k^2 is defined as:

$$k^2 = 5\, M_p{}^2 - 6\, M_p\, \alpha + \alpha^2 \qquad (4)$$

The yield surface defined by Equation 3 and the yield stresses of AC dense Aio sand obtained by Yasufuko et al. (1991) are compared in Figure 2. Values of $M_{p,c} = 1.015$ and $M_{p,e} = -0.758$ equal to those initially used for IC sand were substituted in this equation. As with IC sand, while measured and calculated yield stresses agree well on the compression side, the same is not true in TE. Use of $M_{p,e} = -0.5$ equal to that used for IC sand (broken curve) leads to a significantly better match. As with IC sand, this decrease in yield stresses is due to inherent anisotropy, which existed prior to anisotropic consolidation. The current example suggests that inherent anisotropy can be accounted for by appropriate values of $M_{p,c}$ and $M_{p,e}$, and that in the case examined here, these stress ratios were not affected by the stress-induced anisotropy resulting from anisotropic consolidation. It will be shown later that a similar conclusion is reached from the examination of values of M_p measured from UESP's of IC and AC loose sand.

Following the above comparisons, and further verification of Equations 1 and 3 by published stress-strain data (see Imam, 1999), these equations will be used as yield surfaces for sand provided appropriate values are substituted for stress ratios M_p.

Note that for AC sand, we used a stress ratio α equal to that obtained experimentally by Yasufuko et al. (1991). This stress ratio depends on the stress ratio at consolidation (η_c) and is,

in general, not known. A procedure to approximate α from η_c and M_p which are known for given loading condition and soil state, is given by Imam (1999). In this procedure, it is assumed that at the end of anisotropic consolidation, where the mean normal stress is p_c, the tangent to the yield surface in the p-q plane is perpendicular to the line corresponding to stress ratio η_c. Using this assumption and the geometry of the yield surface, a relationship can be obtained for α as a function of η_c and M_p. Further discussion of this subject is beyond the scope of this paper.

YIELD SURFACE OF LOOSE OTTAWA SAND AND ITS RELATIONSHIP TO THE UESP

Establishing the Yield Surface of Loose Ottawa Sand

A series of tests was conducted by Skopek (1994) on very loose samples of moist-tamped (MT) "dry" Ottawa sand . IC samples were first loaded in TC by a hanger which exerted a constant axial load to the top of the sample. The confining pressure was then gradually decreased under the nearly constant deviatoric stress (CDS) until the steady state was reached.

Results of a typical test are shown in Figure 3. Although the confining pressure was decreased substantially between points A and B, very small volume change occurred in this portion of the CDS loading. However, at point B, void ratio started decreasing at high rate and this behavior continued until the steady state was reached at point C. Although not shown here, axial strains developed before point B were very small, but they increased substantially afterwards until the steady state was reached. Similar results were obtained in other CDS tests.

Equation 1, along with results of the aforementioned CDS tests, is used here to obtain the yield surface of loose Ottawa sand. Equation 1 can be used to define a yield surface if M_p and p_c

are known. Figure 4 shows that point B at which volumetric contraction starts is the point at which the loading path reaches the yield surface that was originally established at point A, where the full deviatoric stress was applied. Between points A and B, the sample is unloaded elastically and the void ratio slightly increases; however, compared to the subsequent large contractions, the void ratio will be assumed to remain constant.

From each CDS test, two points similar to A and B, which belong to the same yield surface can be identified. Such yield surface is characterized by values of p_c and M_p corresponding to the state of the soil between A and B. For these IC samples, p_c and M_p for each test can be obtained by fitting Equation 1 to the positions of points A and B. Figure 4 illustrates the determination of p_c and M_p for two of the CDS tests.

Values of p_c and M_p were determined for all the CDS tests on dry sand conducted by Skopek (1994). It was noticed that M_p is related to void ratio of the sample while it was between points A and B. Figure 5 shows that M_p is inversely related to void ratio and that on average, the relationship can be approximated by a straight line. Substituting this linear relationship into Equation 1 leads to the following yield surface for MT, loose, IC Ottawa sand at void ratio e consolidated to p_c and loaded in TC:

$$f = \eta^2 - 5(4.2 - 4.44e)^2 [1 - (p/p_c)^{1/2}] = 0 \qquad (5)$$

Comparison of the yield surface and the UESP of loose Ottawa Sand

Sasitharan (1994) conducted a series of undrained TC tests on samples of Ottawa sand prepared using the same procedure by which Skopek (1994) prepared his MT samples of dry sand. Consolidated void ratios varied from 0.791 to 0.809 and consolidation pressures from 350 to 550 kPa. The UESP of a typical test in which consolidation void ratio and mean normal stress were e_c = 0.805 (Dr= 5%) and p_c = 550 kPa respectively is shown in Figure 6. In this figure, the

yield surface (Equation 5) of a sample having the same values of e and p_c is also shown for comparison. It can be seen that at such loose state, the UESP closely resembles the yield surface of a sample with e and p_c the same as those at which the undrained sample was consolidated.

Another comparison is shown in Figure 7 in which values of M_p obtained from the "dry" CDS tests (Figure 5) are plotted against void ratio, along with data measured from P-UESP's obtained from undrained tests. Results obtained from the two series of tests are in good agreement, suggesting that M_p may be obtained from either method, and providing a further indication of the proximity of the P-YS to the P-UESP.

VARIATION OF M_P WITH VOID RATIO IN OTHER SANDS

Variations of M_p with void ratio measured from UESP's of Syncrude sand and Toyoura sand are shown in Figure 8 . Physical properties of these sands are provided in Table 1. Results shown in Figure 8(a) were measured from tests conducted at the University of Laval (Konrad and Saint-Laurent 1995), the University of Alberta (Cunning et al. 1995), and the University of British Columbia (Vaid et al. 1996). At Laval, sample dimensions (height to width H/D) of 1:1 and lubricated end platens were used, while at the other two universities, sample dimensions of 2:1 and conventional end platens were used. The Laval and the U of A samples were MT, while those of the UBC were water pluviated (WP). Figure 8(a) shows that the results obtained independently in the three universities are remarkably consistent, perhaps because of the small shear strain at which M_p is mobilized. At such strain level, non-uniformities are unlikely to develop, and sample dimensions and end conditions are not expected to influence the results significantly.

The variation of M_p with void ratio measured from TC tests on MT Toyoura sand (Figure 8 (b)) exhibits a trend similar to that of Ottawa sand and Syncrude sand. It is noted that the

Ottawa, Syncrude and Toyoura sands data were measured from tests with consolidation pressures no more than 600 kPa.

VARIATION OF M_P WITH STATE PARAMETER

The state parameter, ψ, was defined for sands by Been and Jefferies (1985) as the difference between the current void ratio "e" and the steady state void ratio "e_{ss}" at the current mean normal stress "p" such that $\psi = e - e_{ss}$. Samples with $\psi > 0$ (e. g. loose sand) contract and those with $\psi < 0$ (e. g. dense sand) dilate when subjected to shearing. At $\psi = 0$, soils exhibits no tendency for volume change upon shearing.

In order to compare values of M_p for different sands in a unified framework, variations of M_p with the state parameter at peak, ψ_p, are examined for the sands investigated so far, and also for Fraser River and Erksak sands. Figure 9 shows the Steady State Lines (SSL's) of these sands used in the determination of ψ_p, and Table 1 provides their physical properties. The SSL of Toyoura sand was obtained by fitting a polynomial to the Ishihara (1993) data.

Figure 10 shows these variations. From this figure, it may be noticed that:

1. An almost unique relationship exists between M_p and ψ_p for the sands investigated regardless of sand type. The slopes of variation of M_p with ψ_p, namely $k_\psi = \frac{dM_p}{d\psi_p}$, obtained from the different sands are similar.

2. For the predominantly quartzic sands investigated here, the stress ratio M_p at $\psi_p = 0$, denoted by M_μ here, varies between approximately 0.75 and 0.95 with an average of about 0.82. These values correspond to mobilized friction angles between 19.5 and 24 and an average of 21.2

degrees, which are close to the typical variation of the inter-particle friction angle (φ_μ) of quartzic sands (see Procter and Barton, 1974).

3. The stress ratio M_p is higher than M_μ when $\psi_p < 0$ (i.e. in denser, dilative sand) and lower than M_μ when $\psi_p > 0$ (i. e. in looser, contractive sand).

4. The lowest value of M_p, which was measured from tests in which sand experienced complete liquefaction with zero residual strength, is about 0.5. This value corresponds to a friction angle as low as 12 degrees, which is significantly smaller than φ_μ of quartzic sands.

5. In the rounded Ottawa and Erksak sands, the maximum value of M_p, which was measured from tests in which sand just started to exhibit a peak in its UESP, is close to M_μ and occurs at ψ_p close to zero. In the more angular Syncrude and Fraser River sands, this maximum is larger than M_μ and occurs at $\psi_p < 0$.

Undrained tests on loose sands have frequently shown that the rate of development of shear strain is very small before M_p is reached, but it increases substantially afterwards (see e. g. Symes et al. 1984; Doanh et al., 1997). In high confining pressure tests (Bopp and Lade 1997), the shear strains developed before M_p is reached increase with the confining pressure and decrease with the strength of the soil grains, indicating that at high pressures, this shear strain is affected by particle crushing. These observations are consistent with the notion that the strains developed before the stress ratio M_p is reached are the small strains needed to mobilize the shear stresses required for the initiation of gross inter-particle slip. These small strains are followed by the large strains resulting from gross inter-particle slip when stress ratio M_p is exceeded.

The variation of M_p with ψ_p shown in Figure 10 can be approximated by the following relationship:

$$M_p = M_\mu - k_\psi \psi_p \qquad (6)$$

Values of k_ψ for each of the sands investigated, and for all the sands are shown in Figure 10.

THE RELATION OF M_P WITH SOIL STRENGTH AND DILATANCY

Been and Jefferies (1985) showed that the maximum dilatancy of sands decreases with ψ and Jefferies (1993) approximated the variation by a straight line. Wood et al. (1994) expressed the maximum attainable stress ratio at failure, M_f, at the current state parameter ψ by the following equation:

$$M_f = M_{cv} - k_f \psi \tag{7}$$

in which M_{cv} is the constant volume (critical or steady state) stress ratio, and k_f is a material parameter.

Equation 7 has the same form as Equation 6 for M_p. However, at $\psi = 0$, when sand has no tendency for volume change, the mobilized stress ratio obtained from Equation 6 is $M_p = M_\mu$, while that obtained from Equation 7 is $M_f = M_{cv}$. This observed difference may be attributed to the difference between soil conditions at the P-UESP and at failure. Failure is reached while soil is experiencing shear deformation and is in motion; whereas M_p is reached when soil is on the verge of gross inter-particle slip, but is not experiencing such slip yet. In the latter case, if soil has no tendency for volume change, a stress ratio corresponding to the inter-particle friction angle φ_μ is mobilized.

Equations 6 and 7 are also similar to the following form of stress-dilatancy relationship suggested by Nova and Wood (1979):

$$\eta = M_{cv} - \mu d \tag{8}$$

in which η is the current stress ratio, μ is a positive material constant, and $d = \frac{dv}{d\varepsilon}$ is soil dilatancy. Similar to Equations 6 and 7, Equation 8 suggests that the current mobilized stress ratio η increases linearly with soil dilatancy.

Using Equations 6 and 7 for TC, and assuming that the same friction angle φ_m is mobilized in TC and TE, stress ratio M_e in TE can be obtained from stress ratio M_c in TC using $M_e = -3M_c/(3+M_c)$.

Variations of M_p and M_f with ψ obtained using the method explained above are plotted in Figure 11. In this figure, values of $k = 4.6$ and $M_\mu = 0.82$ (obtained from Figure 10) were substituted in Equation 6, and values of $k = 3.5$ (obtained by Jeffries, 1993) and $M_{cv} = 1.2$ were substituted in Equation 7.

It may be noticed from Figure 11 that if the same φ_m is mobilized in TC and TE, smaller slopes of variations of M_p and M_f with ψ will result in TE compared to TC. Such decrease in slope is consistent with the measured variations of M_p discussed in the next section .

VARIATION OF M_P WITH VOID RATIO IN COMPRESSION AND EXTENSION

In Figure 12(a), the variation of M_p with void ratio is shown for Toyoura sand sheared in TC and TE. Values of M_p measured from TE generally plot below those of TC, and the slope of variation is somewhat smaller in TE. The same data plotted in terms of $\tan\varphi_p$ (which corresponds to the coefficient of friction) in Figure 12(b) exhibit closer slopes of variation in TC and TE. These data also indicate that friction angles mobilized at the P-UESP in TE are smaller than

those mobilized in TC; and, the difference is nearly constant (i. e. independent of void ratio) in the sand examined. This difference may be attributed to a constant degree of anisotropy regardless of void ratio. It is noted, however, that the TC and TE samples were prepared by different methods, and this may have a slight effect on M_p and the slope of its variation with void ratio. From Figure 12(b) it may also be noticed that the maximum values of $\tan\varphi_p$, which were obtained from tests in which a peak just started to appear in the UESP, and also the minimum values of $\tan\varphi_p$, which were measured from tests exhibiting complete liquefaction with zero residual strength, are close to each other in TC and TE.

The decrease in the mobilized friction angle at the P-UESP in TE compared to TC is similar to the decrease in the mobilized friction angle at the P-YS in TE observed previously in dense Aio sand. Unlike the results shown in Figure 12, which were obtained from undrained tests, stress ratios at the P-YS of dense Aio sand were obtained by direct determination of yielding stresses from stress-strain data.

EFFECT OF MEAN NORMAL STRESS

At higher mean normal stresses, the simple, approximately linear relationship between M_p and ψ, or M_p and void ratio is no longer valid. Toyoura sand data for consolidation pressures from 100 to 3000 kPa are shown in Figure 13(a). Values of M_p measured from the high-pressure tests ($500<p_c<3000$ kPa) are smaller than those measured from the normal range of pressures ($500 \geq p_c$). It was shown earlier that M_p increases with increase in the dilative tendency of the soil. The decrease in M_p due to increase in confining pressure is consistent with the decrease in soil dilatancy at higher confining pressures reported frequently in the literature (see e. g. Bolton 1986).

Figure 13(a) indicates that increase in consolidation pressure causes decrease in the void ratio corresponding to a certain M_p. If this decrease in void ratio results from sand compression, substituting void ratios measured at different mean normal stresses with a "reference void ratios," e_r, corresponding to a common "reference pressure," p_r, should eliminate the effects of differences in the confining pressures at which M_p is measured. For sand at a given void ratio "e" and consolidation pressure "p", e_r is obtained by moving along the current normal consolidation line (NCL) to the point corresponding to p_r.

Unique CSR line (Vaid et al., 1985) and instability line (Lade, 1992) for samples prepared at the same initial void ratio are equivalent to selecting a very small value for p_r such that e_r becomes practically equal to the initial void ratio e_i at which the sample was prepared before consolidation. In this case, all samples prepared at the same e_i will lie on the same NCL and will have the same e_r. Such samples will have the same M_p regardless of the confining pressures to which they are subsequently subjected.

A difficulty in the determination of e_r, however, is that the compression behavior of sand is complex, and it is not easy to analytically define sand compressibility at various void ratios and confining pressures using simple relationships. A simplified version of a comprehensive compression model suggested by Pestana and Whittle (1995) is used here to define the NCL of sand. In this simplified model, which is given by the following equation, only one material parameter is used to define NCL's of samples with different initial void ratios e_i:

$$\ln (e/e_i) = - e_i^{2.5} C (p/p_a) \qquad (9)$$

in which e is the current void ratio; p and p_a are the current and atmospheric pressures respectively; and, C is a material parameter representing sand compressibility.

In order to obtain e_r, current values of (e , p) should first be substituted in Equation 9 to obtain the initial void ratio e_i. This e_i is then inserted in Equation 9 again along with the selected value of p_r to determine e_r. For a very small p_r (e. g. p_r = 1 kPa), e_r becomes practically equal to e_i and is obtained by following only the first step explained before.

Data used in Figure 13(a) are re-plotted with respect to e_i in Figure 13(b). It may be noticed that values of M_p measured from the high-pressure tests plot very close to those obtained from the other tests.

If ψ is used as an abscissa, on the other hand, values of M_p measured from the high confining pressure tests plot "above" those from the other tests as shown in Figure 14(a). At high pressure, the SSL in the e-ln p plane bends sharply towards the p axis (see eg. the SSL of Toyoura sand in Figure 9), resulting in unusually high values of ψ for loose sand. The increase in the slope of the SSL at high pressures is often attributed to particle crushing, which results in increase in sand compressibility. Use of ψ to describe soil behavior in this region is questionable (Jefferies and Been, 2000). To correlate M_p with ψ for a wider range of pressures, change in sand compressibility at various pressures should be incorporated in the definition of ψ. We define a "reference state parameter," ψ_r, corresponding to a reference pressure p_r, in which change in void ratio due to compressibility is accounted for by a term (e_r - e) subtracted from ψ such that:

$$\psi_r = \psi - (e_r - e) \tag{10}$$

In this equation, ψ is the state parameter at the current values of p and e. The reference void ratio e_r can be obtained using Equation 9 as explained before. As stated earlier, for small values of p_r, e_r is very close to the initial void ratio e_i. Similarly, the reference state parameter corresponding to small p_r will be referred to as the "initial state parameter" ψ_i. Because of ease of determination, we will use e_i and ψ_i in our correlations with M_p.

In Figure 14(b), the data shown in Figure 14(a) are plotted in terms of ψ_i. It may be noticed that the scatter in the data has decreased significantly.

CORRELATING THE VARIATION OF M_P WITH VOID RATIO

Although because of physical considerations, tan ϕ_p was used previously to represent mobilized friction at the P-UESP, it is more convenient to correlate sin ϕ_p with void ratio since it can be related to M_p by the following simple relationships:

$$\text{(a) } M_{p,c} = \frac{6\sin\varphi_p}{(3-\sin\varphi_p)} \qquad \text{(b) } M_{p,e} = \frac{6\sin\varphi_p}{(3+\sin\varphi_p)} \tag{11}$$

The variation of sin ϕ_p with the void ratio of Toyoura sand is shown in Figure 15(a). For the range of friction angles within which ϕ_p normally varies, sin ϕ_p can be related to void ratio by an approximately linear relationship similar to that observed for tan ϕ_p, and we have:

$$\sin\varphi_{p,c} = \sin\varphi_\mu - k_p\,(e_i - e_\mu) \qquad \text{for TC} \tag{12-a}$$

$$\sin\varphi_{p,e} = \sin\varphi_\mu - a_p - k_p\,(e_i - e_\mu) \qquad \text{for TE} \tag{12-b}$$

in which $\varphi_{p,c}$ and $\varphi_{p,e}$ are the friction angles at the P-UESP obtained from TC and TE tests respectively, e_μ is the initial void ratio corresponding to φ_μ, k_p is the slope of variation, and a_p is the difference between sin φ_p obtained from TC and TE tests on samples with $e_i = e_\mu$ (Figure 15(b)) and may be considered as a measure of soil inherent anisotropy. In Toyoura sand, the slope k_p obtained from TC and TE tests were close to each other, but different slopes may be used if experimental results necessitated. Note that in using Equation 6, M_μ should be obtained directly from test data similar to those shown in Figure 10. In Equation 12, however, φ_μ is

selected as a reference value which, together with e_μ, is used to define the line by which the variation of $\sin\varphi_p$ with void ratio is approximated.

Equation 6 can be re-written in terms of ψ_r in order to make it applicable to a wider range of pressures:

$$M_p = M_\mu - k_{\psi,r}\,\psi_r \qquad (13)$$

in which $k_{\psi,r}$ is the slope obtained from a plot of M_p vs. ψ_r.

When confining pressures vary within a limited range, it may not be necessary to use e_i or ψ_r in Equations 12 and 13 respectively, and use of e_c or ψ can provide sufficiently accurate correlations. Because of the difficulties associated with the determination of steady state lines, using e or e_i is often more convenient than using ψ or ψ_r. Therefore, in the correlations that follow, we will use e_i or e, depending on the range of pressures involved.

The relationships of M_p or $\sin\varphi_p$ with e_i or e_c obtained so far are consistent with the general trend of the TC results presented by of Lade (1993) and Yamamuro and Lade (1997), and the TE results of Vaid and Thomas (1995). The current study further indicates that $\sin\varphi_p$ (or M_p) depends on e_i in both TC and TE, and that for the sands investigated here, a unique relationship exists between M_p and state parameter. Straight lines were used here to approximate the relationships.

Unique instability lines (Lade and coworkers, 1993, 1997) and CSR lines (Vaid and coworkers, 1985, 1995, 1999) have often been obtained from tests on samples prepared by dry deposition (DD) or water pluviation (WP). Using these methods, the range of achievable void ratios at which a peak appears in the UESP and therefore, values of M_p measured from tests on samples at such void ratios, is limited. Looser samples can be prepared by moist tamping (Ishihara, 1993), and consequently, a wider range of M_p can be measured. Differences in the

ranges of data obtained from theses preparation methods can be noticed from Figure 8 and Figure 16. While there are different ideas regarding the preparation method that can best resemble real field deposition processes and void ratios (see eg. Vaid 1999; Lade and Yamamuro 1997), the aforementioned data reflect a generally consistent variation of M_p with void ratio regardless of preparation method.

EFFECT OF ANISOTROPIC CONSOLIDATION AND PRE-SHEARING

Values of M_p measured from MT and DD Toyoura sand are shown in Figure 16. These results were measured from tests on IC and AC samples subjected to loading at various values of $K_0 = \sigma_h / \sigma_v$. All anisotropic consolidations were in compression (i.e. $\sigma_v > \sigma_h$) but undrained shearing was in TC or TE.

Except for the data point with $\eta_c = 0.64$ in Figure 16-a, values of M_p measured from IC and AC sand are generally the same, indicating that in these cases, anisotropic consolidation has not affected M_p. This result applies to both the TC and TE data, and is similar to that reported by Vaid and Chern (1985) and Doanh et al (1997). Note that although the data shown in Figure 16-b were obtained from three different sources, there is very good agreement among them, as was in the case for Syncrude sand (Figure 8).

Stress ratios at the P-YS of dense Aio sand examined previously exhibited similar independence with respect to anisotropic consolidation, although they were derived from direct determination of yielding stresses rather than UESP's.

The AC sample with $\eta_c = 0.64$ in Figure 16(a) exhibited an M_p which is larger than that of an IC sample with the same void ratio. The sample was consolidated to $\eta_c > M_p$ of an IC sample,

and consequently, M_p increased to a value larger than that of an IC sample. Similar results were observed by di Prisco et al. (1995) and Doanh et al. (1997).

Vaid et al (1989) showed that pre-shearing of loose sands to stress ratios smaller than the CSR does not affect the CSR regardless of whether pre-shearing is applied in TC, TE, monotonic or cyclic loading. However, large pre-shearing beyond the CSR increased the CSR in the direction of pre-shearing. When undrained loading was applied in the same direction as the previous large pre-shearing (eg. pre-shearing and undrained loading were both in TC or both in TE), the slope of the CSR line increased and the sample became more dilative. However, when undrained shearing was in a direction opposite to that of pre-shearing, the slope of the CSR decreased and the sample exhibited higher contraction during undrained loading.

The changes in M_p due to anisotropic consolidation or pre-shearing discussed above are similar to the kinematic hardening of yield surfaces resulting from anisotropic consolidation or shearing. It can be shown (Imam et al., 2002) that the locus of M_p in octahedral plane represents a rounded triangle similar to the shape of yield surfaces obtained from stress-strain data. Schematic representations of such shape and the locus of stress ratios M_{PT} at Phase Transformation (PT) are shown in Figure 17. The PT was defined by Ishihara et al. (1975) as the condition at which sand behavior changes from contractive to dilative.

Anisotropic consolidation or pre-shearing shifts the yield surface in the direction of the shearing load (see eg. Cambou and Lanier, 1988; di Prisco et al, 1993). When anisotropic consolidation and pre-shearing are applied at stress ratios smaller than the M_p of IC sand, the locus of stress ratios M_p remains unchanged and consequently, values of M_p in TC and TE will not be affected. However, when they are applied at stress ratios higher than M_p, the locus of M_p shifts in the direction of shearing and consequently, the current M_p increases in this direction and

decreases in the opposite direction. From the available test data (eg. Vaid et al., 1989; di Prisco et al., 1995; Doanh et al., 1997) it can be concluded that such movement of the locus of M_p takes place regardless of whether shearing is due to anisotropic consolidation, pre-shearing in TC or TE, or cyclic loading. Yield surfaces obtained from stress-strain data exhibit similar translations, known as kinematic hardening in soil plasticity, in the direction of anisotropic consolidation and/or pre-shearing (see eg. Cambu and Lanier, 1988; di Prisco et al., 1993).

It can be noticed from Figure 17 that when the locus of M_p is translated in the compressional direction, it becomes closer to the locus of M_{PT} in compression and farther in extension. Since in undrained loading, sands exhibit strain softening (ie. loss of shear strength) in stress ratios between M_p and M_{PT}, the region of stress space over which strain softening takes place becomes smaller on the compression side (ie. sand becomes more dilative in compression) and larger on the extension side (ie. becomes more contractive in extension). The opposite is true if pre-shearing is applied in extension. These results are consistent with the observations of Vaid et al. (1989) discussed previously.

SUMMARY AND CONCLUSIONS

Experimental evidence presented in this paper suggest that for very loose sand, the shape of the yield surface closely resembles the shape of the undrained effective stress path (UESP) and the stress ratio M_p at the peak of the UESP is affected by similar factors, and varies in the same way, as the stress ratio at the peak of the yield surface (P-YS). These observations are consistent with the propositions of Nova and Hueckel (1978) and Lade (1992). The UESP of loose sand can therefore be used to approximate material parameters which appear in the definition of yield surfaces for sand. Variations of M_p with void ratio and consolidation stresses were examined for

TC and TE loading using published test data. These variations were compared with previous studies and then modeled by analytical relationships.

Variation of M_p with state parameter ψ was also examined. A unique relationship between M_p and ψ was observed for the sands investigated regardless of sand type. This relationship revealed that inter-particle friction and soil dilatancy are two major factors affecting mobilized stresses at the P-UESP. Comparison of data from TC and TE tests, and examination of effects of pre-shearing and anisotropic consolidation indicated that inherent and stress-induced anisotropies affect the stress ratio at the P-UESP in the same way as they affect the yielding stresses. Effects of the intermediate principal stresses and direction of loading on M_p are examined elsewhere (Imam et al. 2002). Analytical equations obtained here and elsewhere for the variation of M_p have been used in defining yield surfaces and modeling the constitutive behavior of sand. These yield surfaces can also be used in qualitative assessments of the susceptibility of loose sands to flow liquefaction (see Imam, 1999).

ACKNOWLEDGEMENT

This study was supported in part by the Natural Sciences and Engineering Research Council of Canada, NSERC. The first author would also like to acknowledge the support of the MCHE of Iran during his PhD studies.

NOTATION:

a_p = Difference between $\sin\varphi_p$ of sand with $e_i = e_\mu$, in triaxial compression and extension

C = Material parameter for sand compressibility

$d = \frac{dv}{d\varepsilon}$ Soil dilatancy

Dr, Dr_i = Current, and initial (preparation) relative densities

e, e_c, e_{ss} = Current, consolidation, and steady state void ratios

e_i = Initial void ratio, measured at preparation of sand sample

e_r = Reference void ratio corresponding to reference pressure p_r

e_μ = Initial void ratio corresponding to mobilized friction angle φ_μ at peak of undrained effective stress path

$K_0 = \sigma_h / \sigma_v$ Coefficient of lateral earth pressure

k_f = Slope of variation of M_f with state parameter

k_p = Slope of variation of $\sin\varphi_p$ with void ratio

k_ψ, $k_{\psi,r}$ = Slopes of variation of M_p with state parameter ψ, and reference state parameter ψ_r

M_c, M_e = Stress ratios q/p in triaxial compression, and extension

M_{cv}, M_f = Stress ratios q/p at constant volume shearing, and at failure

M_p = Stress ratio q/p at peak of undrained effective stress path (P-UESP)

$M_{p,c}$, $M_{p,e}$ = Stress ratios M_p in triaxial compression, and triaxial extension

M_μ = Stress ratio q/p corresponding to inter-particle friction

p, p_a = Effective mean normal stress, and atmospheric pressure

p_c, p_α = Effective mean normal stress at consolidation, and at yielding under stress ratio α

p_r = A reference value of effective mean normal stress

$q = \sigma_1 - \sigma_3$ Deviatoric stress

α = Stress ratio q/p at which tangent to yield surface is perpendicular to p-axis

$\varphi_{p,c}$, $\varphi_{p,e}$ = Friction angles at peak of undrained effective stress path in TC, and TE tests

φ_i = Friction angle corresponding to "Instability Line"

φ_m, φ_μ = Mobilized, and inter-particle friction angles

η, η_c = Current, and consolidation ratios q/p

μ = Material parameter in Nova and Wood's dilatancy relationship

ψ, ψ_p = State parameter, and state parameter at the peak of undrained effective stress path

ψ_r = Reference state parameter corresponding to reference pressure p_r

ψ_i = Initial state parameter before the application of confining pressure (ie. at very small reference pressure)

REFERENCES

Been, K. and Jefferies, M. G. 1985. A state parameter for sands. Geotechnique, **35**(2): 99-112.

Been, K., Jefferies, M. G., and Hachey, J. 1991. The critical state of sands. Geotechnique, **41**(3): 365-381.

Bishop, A. W. 1971. Shear strength parameters for undisturbed and remolded soil specimens. Roscoe Memorial Symposium: 3-58.

Bolton, M. D. 1986. The strength and dilatancy of sands. Geotechnique, **36**(1): 65-78.

Bopp, P. A. and Lade, P. V. 1997. Effects of Initial Density on Soil Instability at High Pressures. Journal of Geotechnical and Geoenvironmental Engineering, ASCE, **123**(7): 671-677.

Cambou, B. and Lanier, J. 1988. Induced anisotropy in cohesionless soil: Experiments and modeling. Comput Geotech, **6**(4): 291-311.

Chillarige, A. V., Robertson, P. K., Morgenstern, N. R., and Christian, H. A. 1997. Evaluation of the in situ state of Fraser River sand. Canadian Geotechnical Journal, **34**(4): 510-519.

Cunning, J. C., Robertson, P. K., and Sego, D. C. 1995. Shear wave velocity to evaluate in-situ state of cohesionless soils. Canadian Geotechnical Journal, **32**: 848-858.

Di Prisco, C., Matiotti, R., and Nova, R. 1995. Theoretical Investigation of the Undrained Stability of Shallow Submerged Slopes. Geotechnique, **45**(3): 479-496.

di Prisco, C., Nova, R., and Lanier, J. 1993. A mixed isotropic kinematic hardening constitutive law for sand. Modern approaches to plasticity ed. D. Kolymbas, Roterdam: Balkema.: 83-124.

Doanh, T., Ibraim, E., and Matiotti, R. 1997. Undrained instability of very loose Hostun sand in triaxial compression and extension. Part 1: Experimental observations. Mechanics of Cohesive Frictional Materials, **2**(1): 47-70.

Hanzawa, H. 1980. Undrained Strength and Stability Analysis for a Quick Sand. Soils and Foundation, **20**(2): 17-29.

Hyodo, M., Tanimizu, H., Yasufuku, N., and Murata, H. 1994. Undrained cyclic and monotonic triaxial behavior of saturated loose sand. Soils and Foundations, **34**(1): 19-32.

Imam, S. M. R., Chan, D. H., Robertson, P. K. and Morgenstern, N. R. 2002. Effect of anisotropic yielding on the flow liquefaction of loose sand. Accepted for publication in Soils and Foundations.

Imam, S. M. R. 1999. Modeling the constitutive behavior of sand for the analysis of static liquefaction. Ph D thesis, University of Alberta.

Ishihara, K. 1993. Liquefaction and flow failure during earthquakes. Geotechnique, **43**(3): 351-415.

Ishihara, K., Tatsuoka, F., and Yasuda, S. 1975. Undrained deformation and liquefaction of sand under cyclic stresses. Soils and Foundations, **15**(1): 29-44.

Jefferies, M. G. 1993. Nor-Sand: a simple critical state model for sand. Geotechnique, **43**(1): 91-103.

Jefferies, M. G. and Been, K. 2000. Implications for critical state theory from isotropic compression of sand. Geotechnique, **50**(4): 419-429

Konrad, J. M., 1993. Undrained response of loosely compacted sands during monotonic and cyclic compression tests. Geotechnique, **43**(1): 69:89.

Konrad, J. M. and Saint-Laurent, S. 1995. Laboratory testing of reconstituted and in-situ frozen specimens-Syncrude tailings sand, CANLEX Technical Report, Phase I, Activity 8C, Universite' Laval.

Lade, P. 1992. Static instability and liquefaction of loose fine sandy slopes. Journal of Geotechnical Engineering ASCE, **118**(1): 51-70.

Lade, P. 1993. Initiation of static instability in the submarine Nerlerk berm. Canadian Geotechnical Journal, **30**: 895-904.

Lade, Poul, V and Yamamuro, Jerry A. 1997. Effects of nonplastic fines on static liquefaction of sands. Canadian Geotechnical Journal, **34**(6): 918-928.

Nova, R. and Wood, D. M. 1978. An experimental program to define the yield function for sands. Soils and Foundations, **18**(4): 77-86.

Nova, R. and Wood, D. M. 1979. A constitutive model for sand in triaxial compression. Int. J. Num. Anal. Meth in Geomech., **3**: 255-278.

Nova, R. and Hueckel, T. 1981. A unified approach to the modeling of liquefaction and cyclic mobility of sands. Soils and Foundations, **21**(4): 13-28.

Pestana-Nascimento, J. M. 1994. A unified constitutive model for clays and sands. Ph D thesis, Massachusetts Institute of Technology.

Pestana, J. M. and Whittle, J. A. 1995. Compression Model for Cohesionless Soils. Geotechnique, **45**(4): 611-631.

Procter, D. C. and Barton, R. R. 1974. Measurement of the angle of interparticle friction. Geotechnique, **24**(4): 581-604.

Sasitharan, S., 1994. Collapse behavior of very loose sands. Ph.D. thesis, University of Alberta.

Skopek, P. 1994. Collapse behavior of very loose dry sand. Ph.D. thesis, University of Alberta.

Sladen, J. A., D'hollander, R. D., and Krahn, J. 1985. The liquefaction of sands, a collapse surface approach. Canadian Geotechnical Journal, **22**: 564-578.

Symes, M. J., Gens, A., and Hight, D. W. 1984. Undrained anisotropy and principal stress rotation in saturated sand. Geotechnique, **34**(1): 11-27.

Vaid, Y. P. and Chern, J. C. 1985. Cyclic and monotonic undrained response of saturated sands. Advances in the art of testing soils under cyclic conditions, ASCE Convention, Detroit, Mich.: 120-147.

Vaid, Y. P., Chung, E. K. F., and Kuerbis, R. 1989. Preshearing and Undrained Response of Sand. Soils and Foundation, **29**(4): 46-61.

Vaid, Y. P. and Thomas, J. 1995. Liquefaction and postliquefaction behavior of sand. Journal of Geotechnical Engineering, **121**(2): 163-173.

Vaid, Y. P., Sivathayalan, S., Eliadorani, A., and Uthayakumar, M. 1996. Laboratory testing at UBC. CANLEX report dated April 1996.

Vaid, Y. P. and Sivathayalan, S. 1999. Fundamental Factors Affecting Liquefaction Susceptibility of Sands. in Physics and Mechanics of Soil Liquefaction (ed. Lade, P., Yamamuro, J.): 105-120.

Verdugo, R. L. 1992. Characterization of sandy soil behavior under large deformation. Ph D thesis, University of Tokyo.

Wood, D. M., Belkheir, K., and Liu, D. F. 1994. Strain softening and state parameter for sand modeling. Geotechnique, **44**(2): 335-339.

Wride, C. and Robertson, P. K. 1997a. CANLEX Phase I and III, data review report.

Wride, C. and Robertson, P. K. 1997b. CANLEX Phase II, Data Review Repot.

Yamamuro, Jerry A. and Lade, Poul, V 1997. Static liquefaction of very loose sands. Canadian Geotechnical Journal, **34**(6): 905-917.

Yasufuku, N., Murata, H., and Hyodo, M. 1991. Yield characteristics of anisotropically consolidated sand under low and high stresses. Soils and Foundations, **31**(1): 95-109.

Yoshimine, M. 1996. Undrained flow deformation of saturated sand under monotonic loading conditions. Ph D thesis, University of Tokyo.

(1) Sand type	(2) Source	(3) Mineralogy	(4) Angularity	(5) D_{50} (mm)	(6) e_{max}	(7) e_{min}	(8) M_{ss}	(9) Steady State Line
Ottawa	Sasitharan (1994)	quartz	rounded to subrounded	0.34	0.82	0.50	1.19	$e = 0.864-0.0168 \ln p$
Toyoura	Ishihara (1993)	75 % quartz ; 25 % Feldespar	subangular	0.17	0.977	0.597	1.24	$e = -0.006348p^3 + 0.0367p^2 - 0.1199p + 0.92548$ (p in MPa) (obtained in current study)
Syncrude	Wride & Robertson (1997a)	95% quartz	angular to subangular	0.15	0.958	0.668	1.19	$e = 0.919 - 0.0152 \ln p$ (for $e > 0.829$)
Fraser River	Wride & Robertson (1997b)	(*) 40 % quartz; 11% feldespar; 45% rock fragments etc.	(*) subangular to subrounded	0.3	1.056	0.677	(*) 1.4	$e = 1.071 - 0.0165 \ln p$ (for $e > 0.979$)
Erksak	Been et al. (1991)	73% quartz; 22% feldespar	rounded to subrounded	0.33	0.753	0.527	1.24	$e = 0.82 - 0.0133 \ln p$ (for $p < 1000$ kPa)

(*) Chillarige et al. (1997)

Table 1 Physical properties of the sands investigated

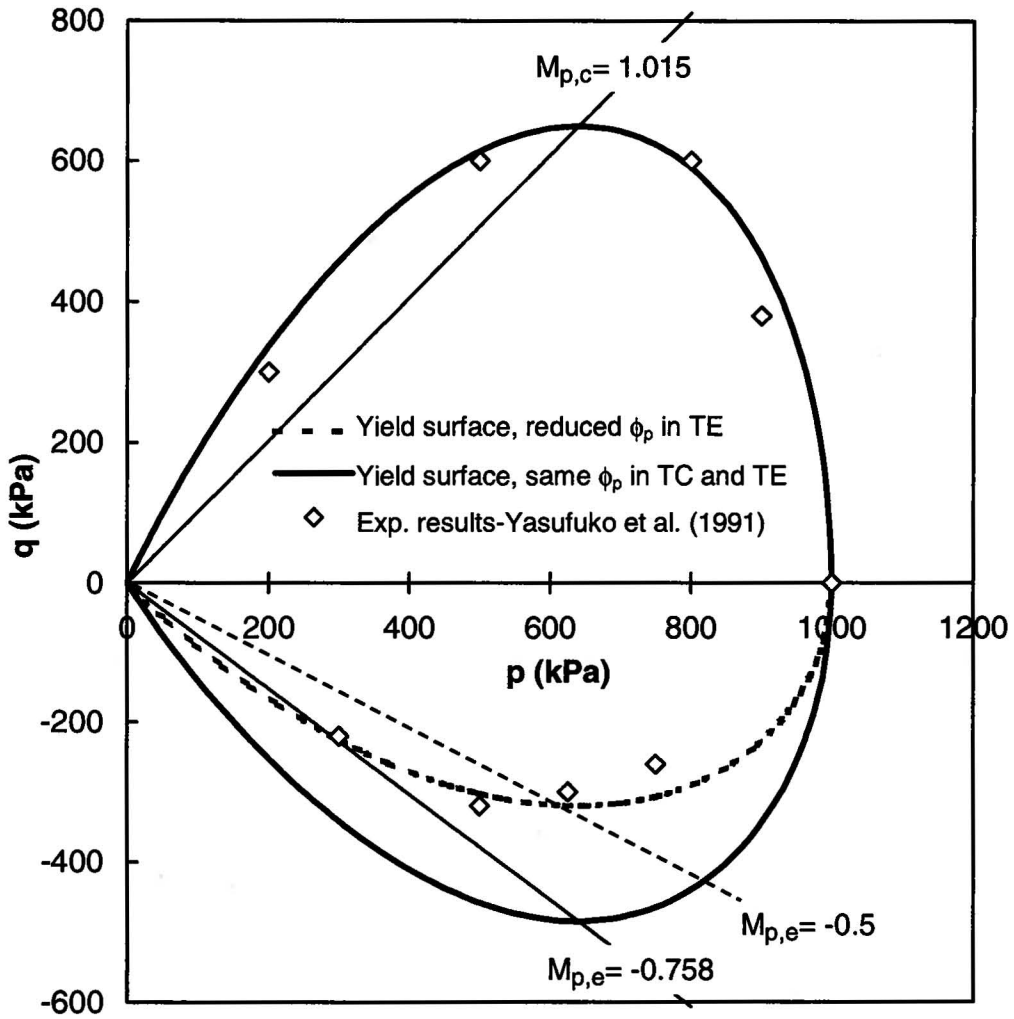

Figure 1 Comparison of the yield surface defined by Equation 1 with the experimental yield stresses of isotropically consolidated dense Aio Sand

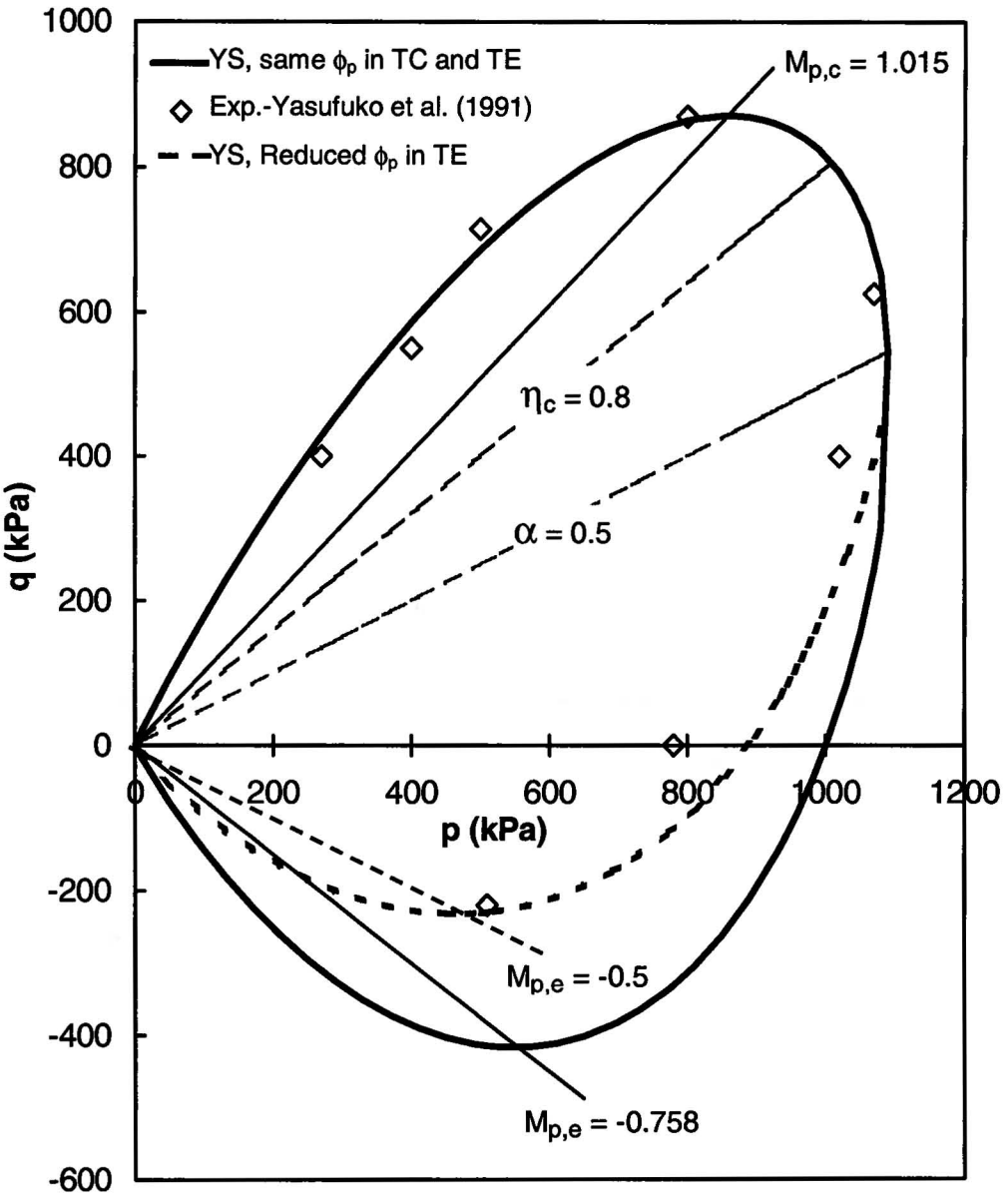

Figure 2 Comparison of the yield surface (YS) defined by Equation 3 with the experimental yield stresses of anisotropically consolidated dense Aio sand

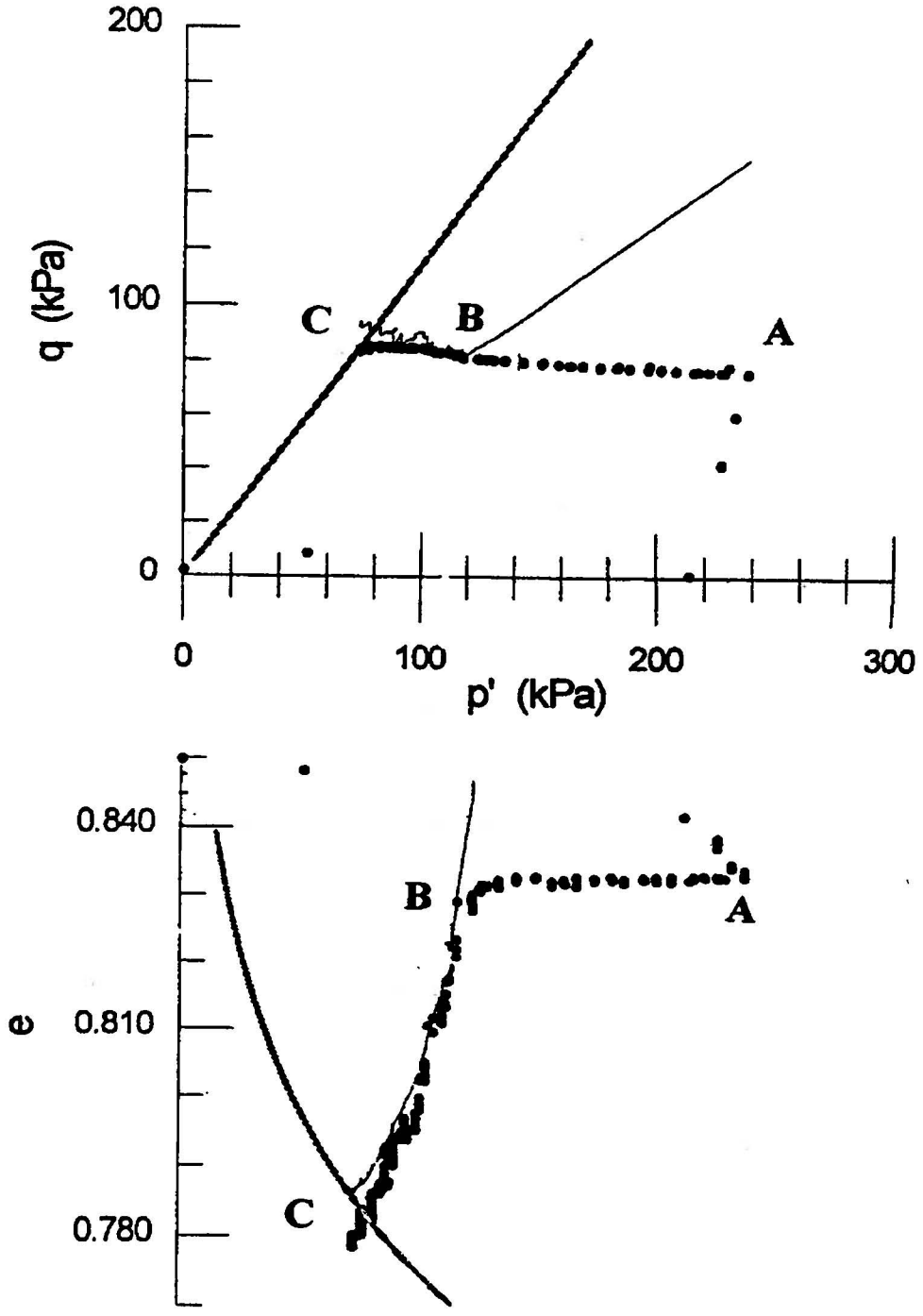

Figure 3 Results of a Constant Deviatoric Stress (CDS) test on very loose dry Ottawa sand (modified after Skopek, 1994)

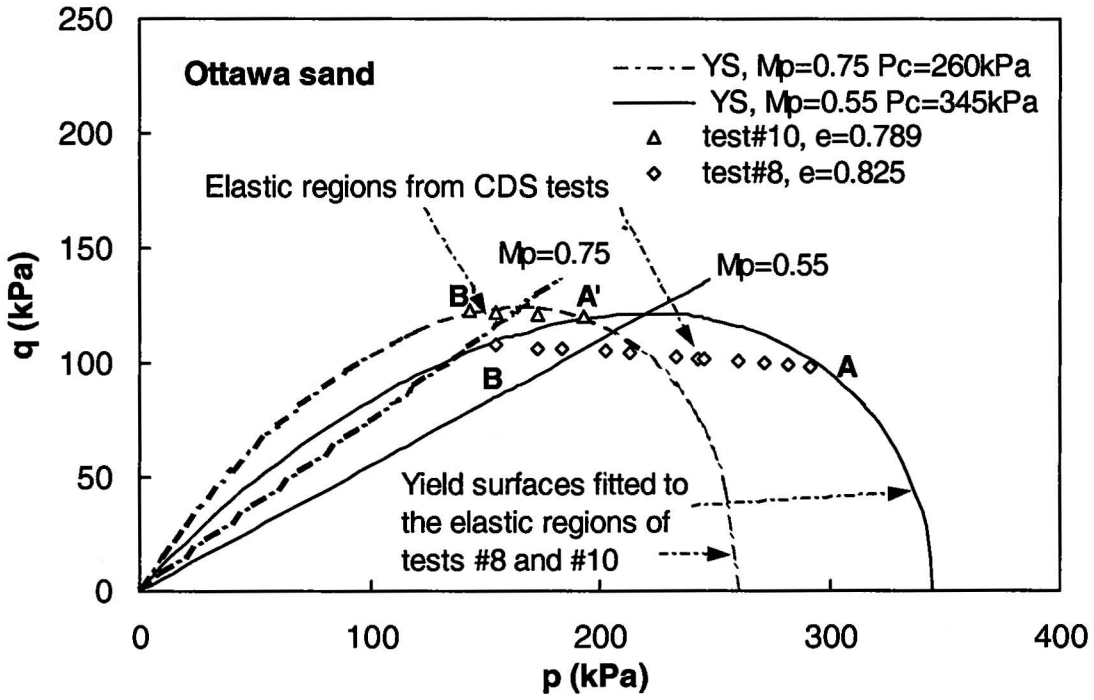

Figure 4 Determination of yielding parameters M_p and p_c from results of CDS tests #8 and #10 (Skopek, 1994) on dry Ottawa sand

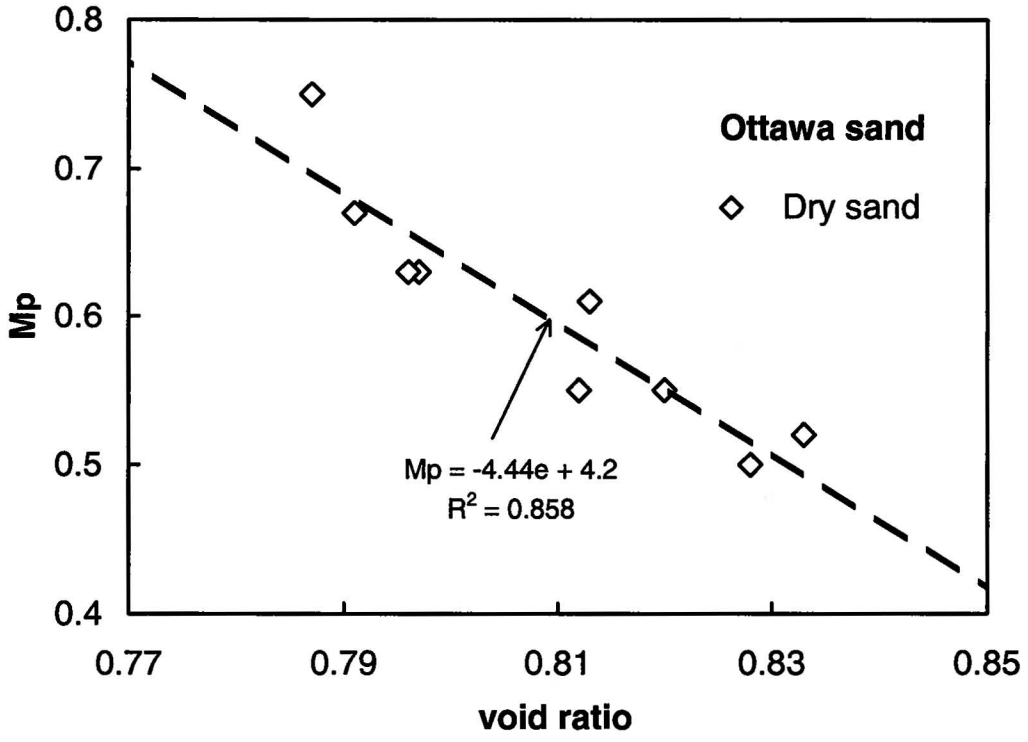

Figure 5 Variation of M_p with void ratio obtained from CDS tests on dry Ottawa sand

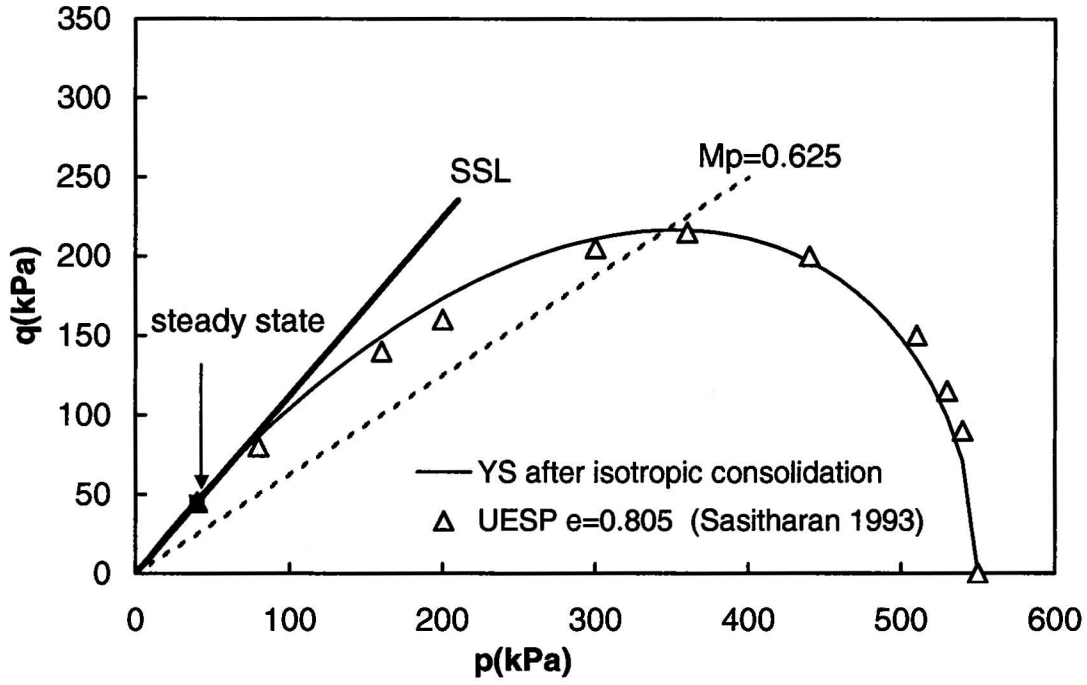

Figure 6 Comparison of the undrained effective stress path (UESP) with the shape of the yield surface of a sample of Ottawa sand consolidated to a void ratio of 0.805 and confining pressure of 550 kPa

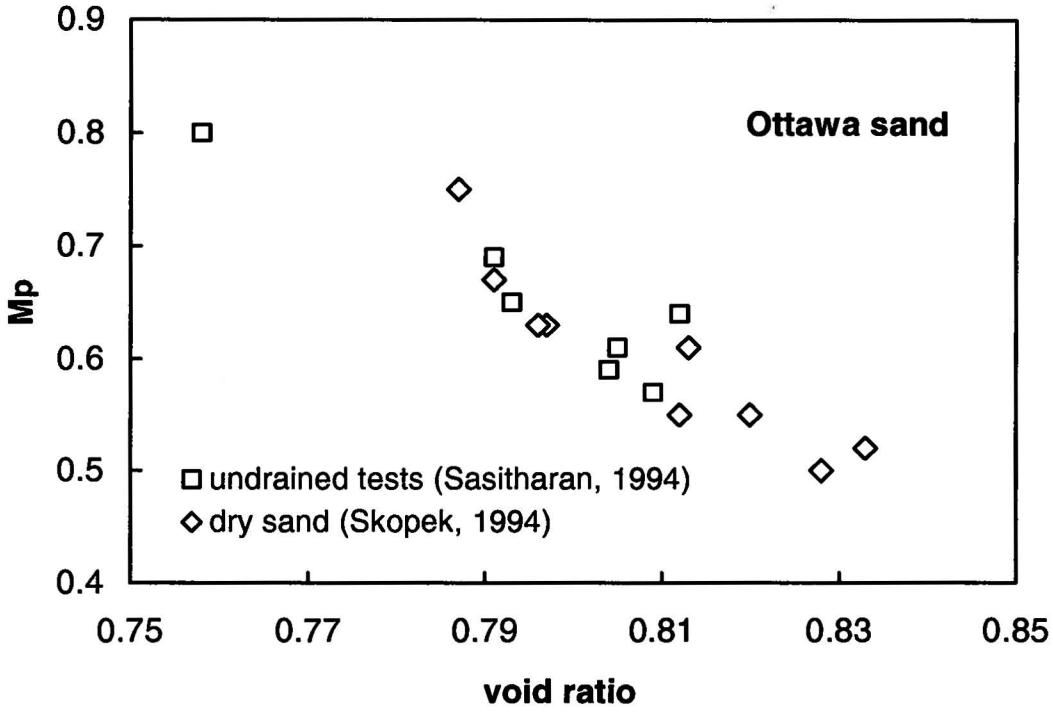

Figure 7 Variation of M_p with void ratio obtained from CDS tests on dry, and undrained tests on saturated Ottawa sand

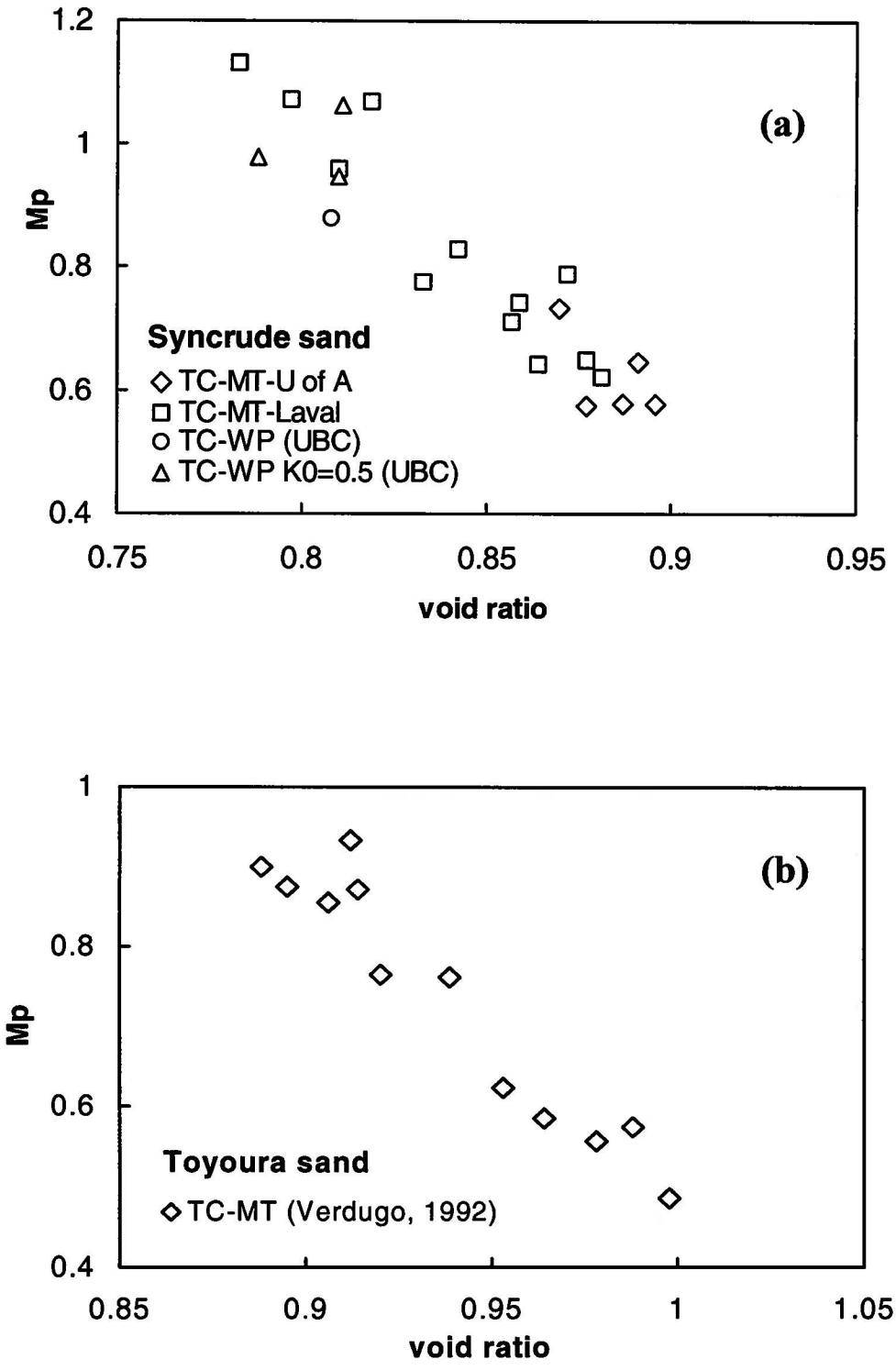

Figure 8 Variation of M_p with void ratio for Syncrude sand and Toyoura sand measured from Triaxial Compression (TC) tests

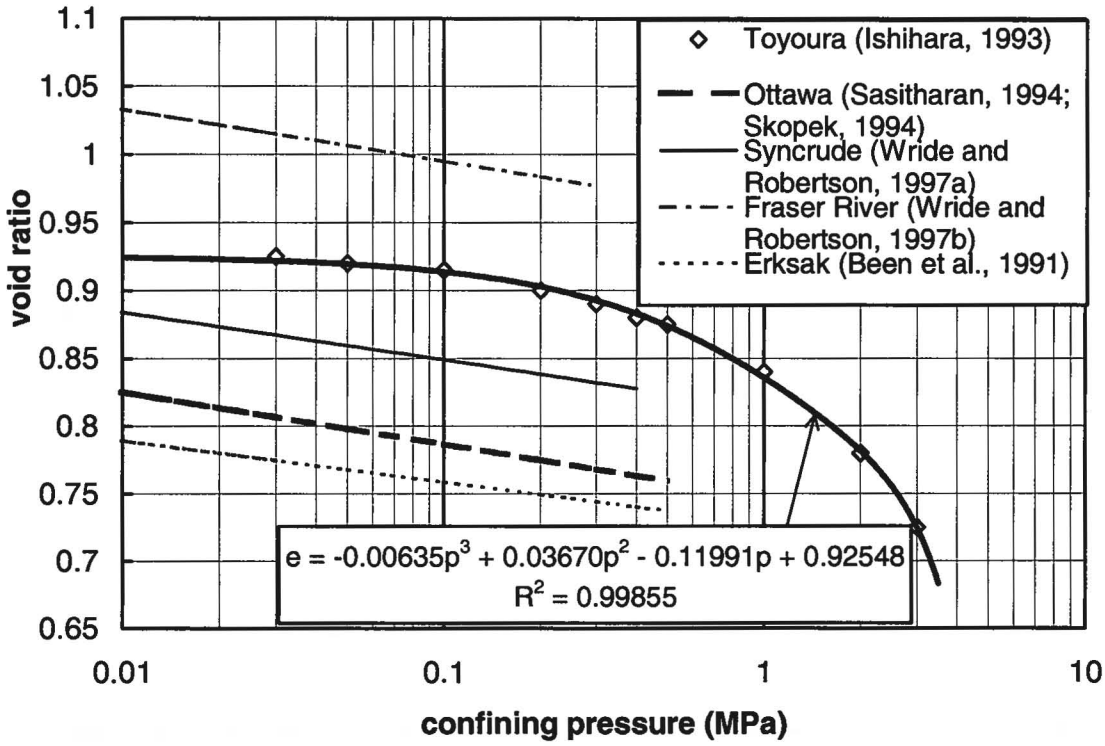

Figure 9 Steady state lines (SSL) of the sands investigated

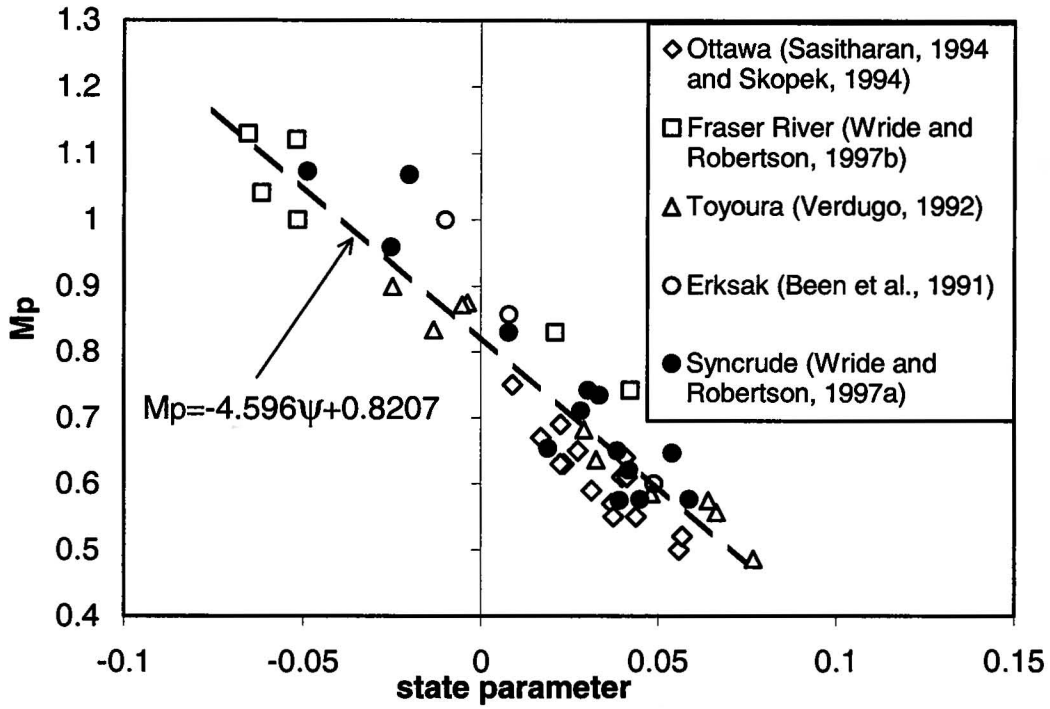

	Ottawa	**Toyoura**	**Syncrude**	**Fraser River**	**Erksak**	**All sands**
Slope k_ψ	4.35	4.14	5.13	3.23	6.70	4.60
Regression coeff. R^2	0.79	0.96	0.89	0.92	0.99	0.86

Figure 10 Variation of M_p with state parameter at the P-UESP in sands consolidated to pressures up to 600 kPa

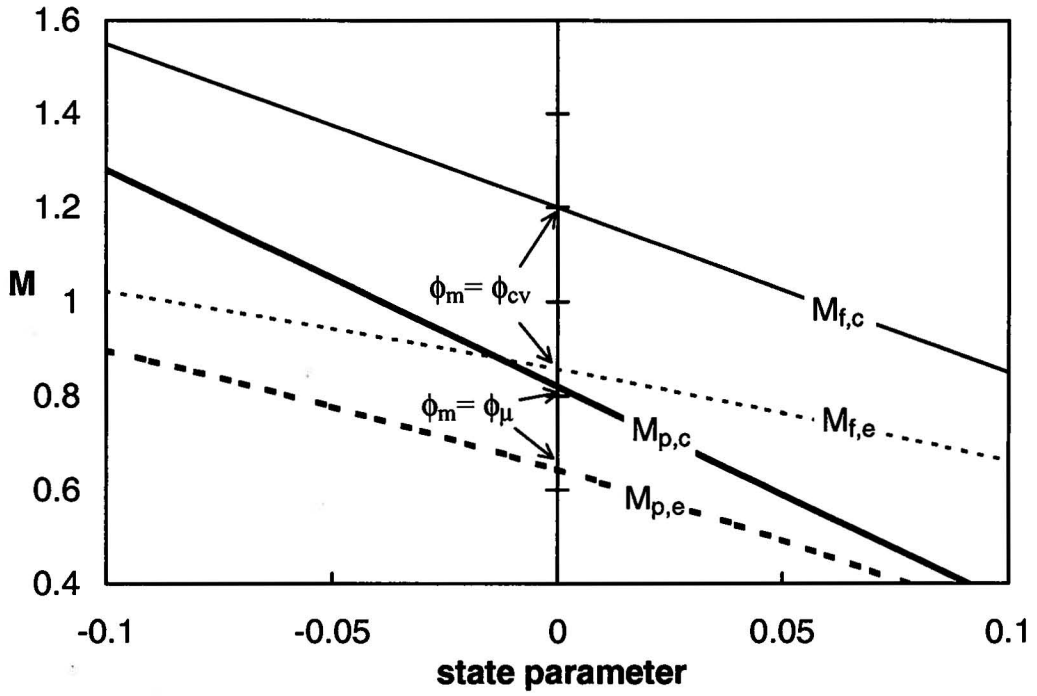

Figure 11 Typical variations of M_p and M_f with state parameter when the same friction angle is mobilized in TC and TE

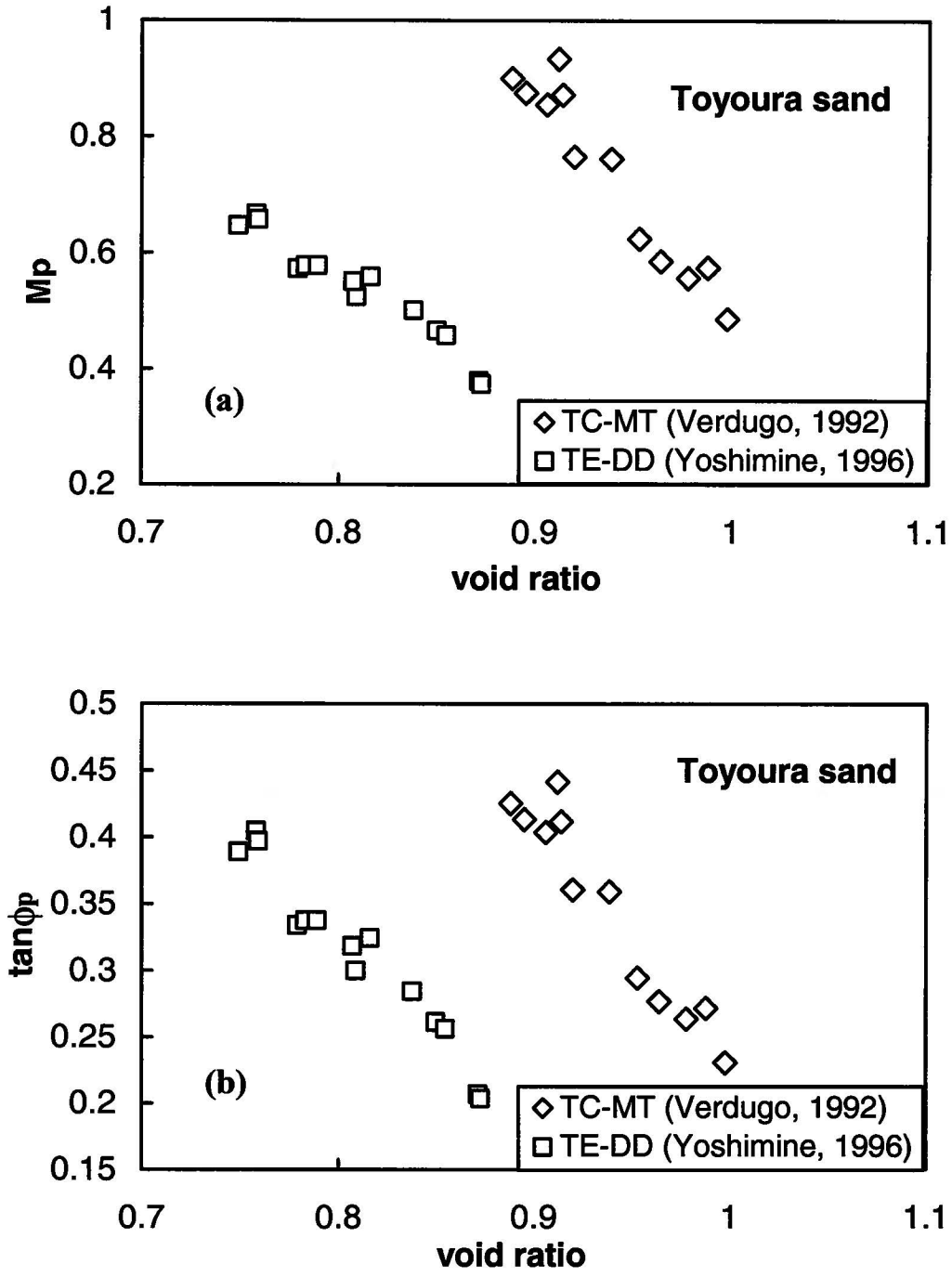

Figure 12 Variation of M_p and $\tan\phi_p$ with void ratio, as obtained from triaxial compression (TC) and triaxial extension (TE) tests

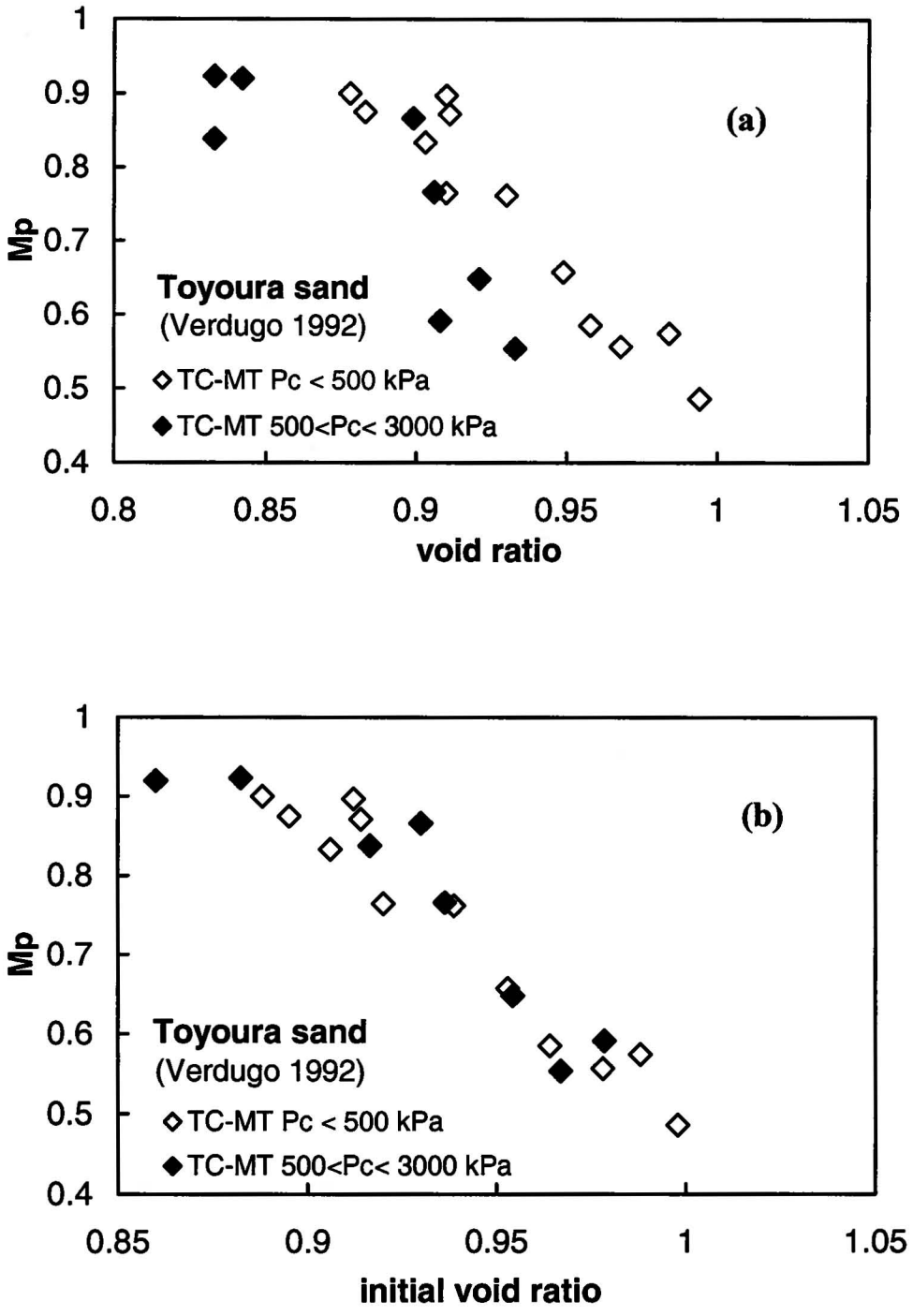

Figure 13 Variation of M_p with void ratio and initial void ratio in the low and high ranges of pressures

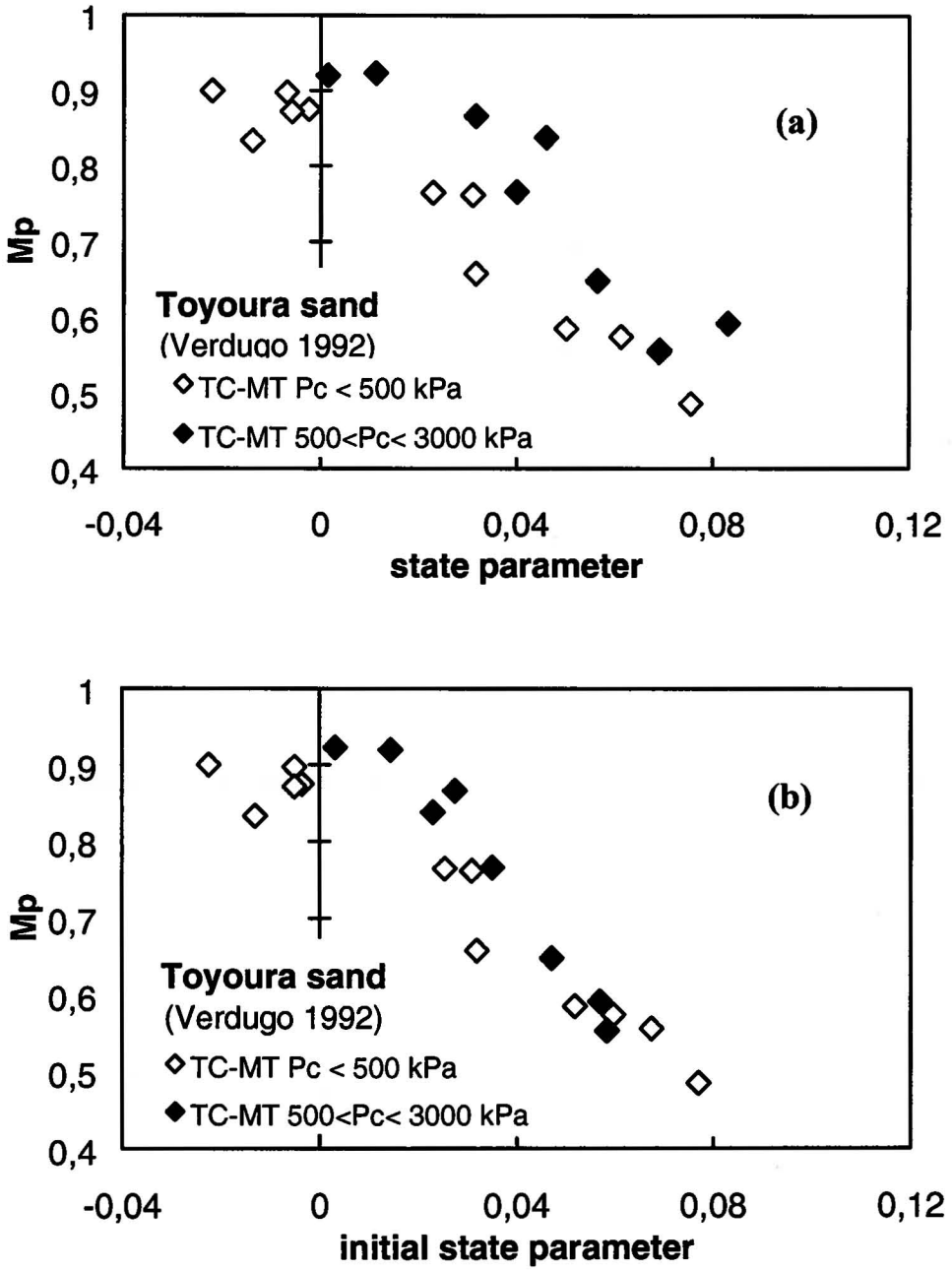

Figure 14 Variation of M_p with state parameter and initial state parameter in the low and high ranges of pressures

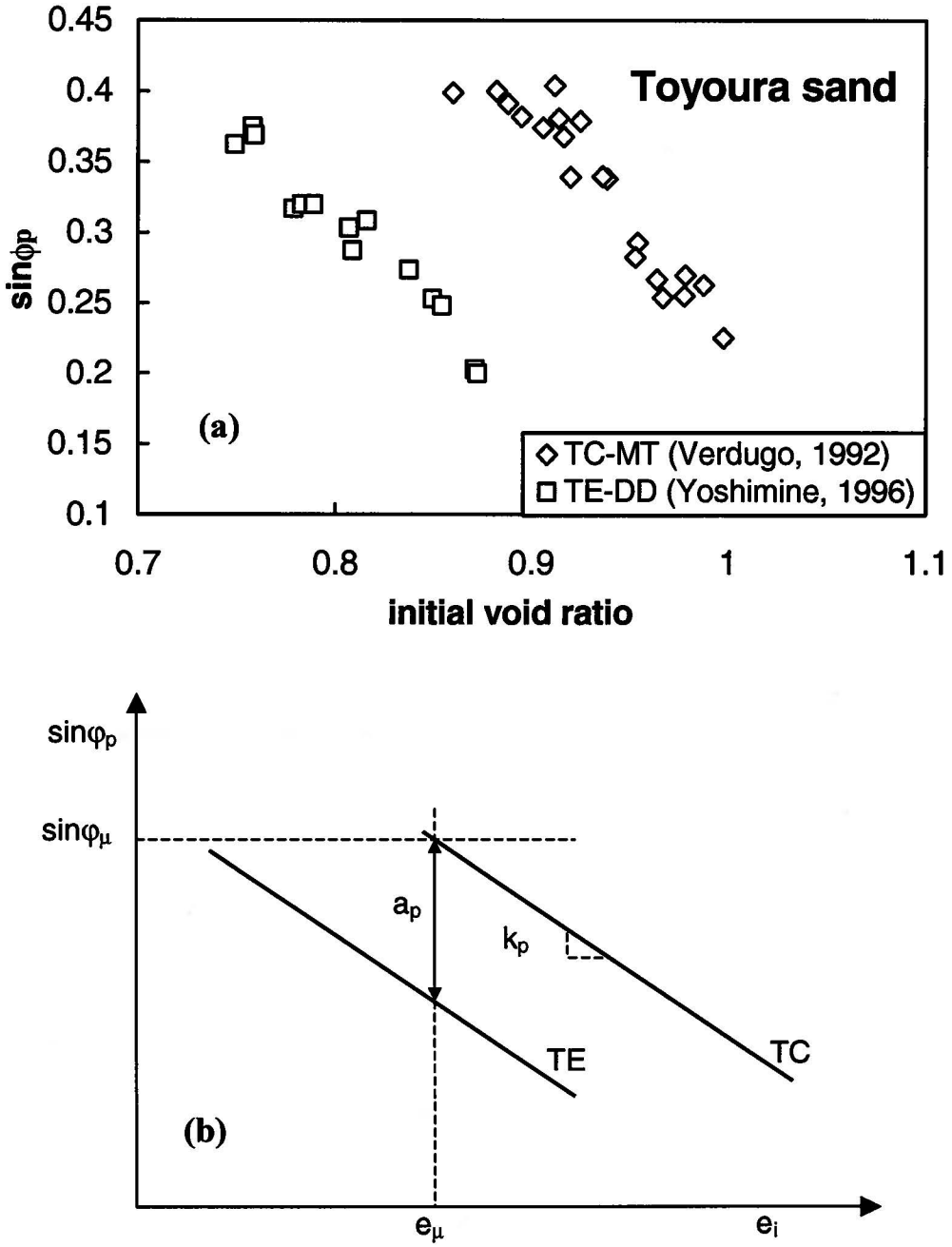

Figure 15 Measured values and schematic representation of variations of $\sin\phi_p$ with initial void ratio for Toyoura sand consolidated to pressures up to 3000 kPa

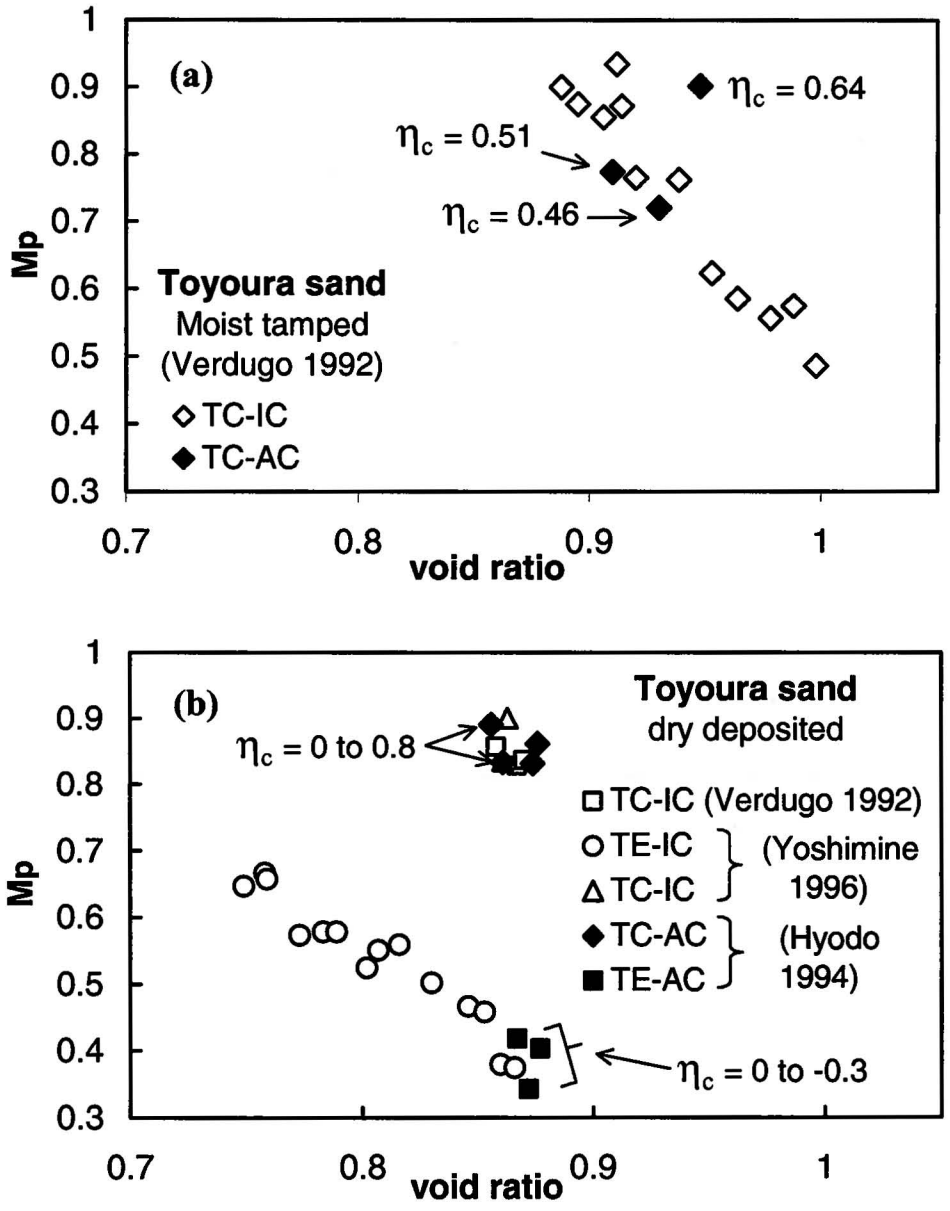

Figure 16 Values of M_p measured from isotropically consolidated (IC) and anisotropically consolidated (AC) sand

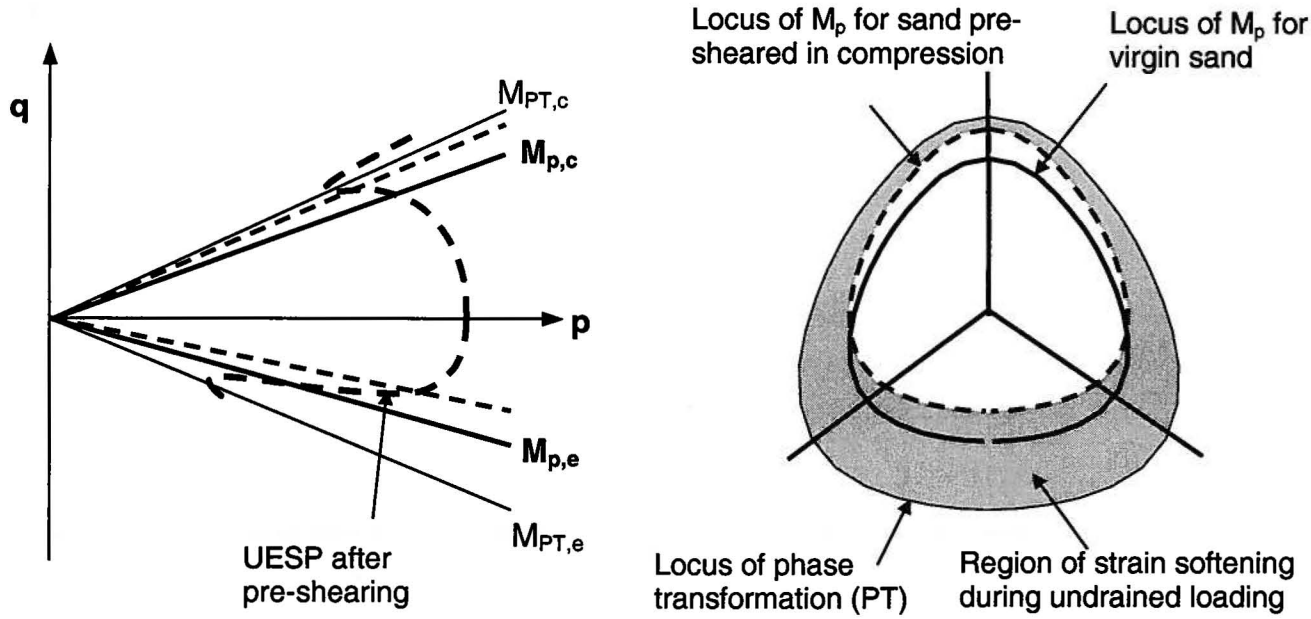

(a) Triaxial plane

(b) Octahedral plane

Figure 17 Schematic representation of changes in $M_{p,c}$ and $M_{p,e}$ due to pre-shearing, and its relationship to kinematic hardening of yield surface